# Estimation of Water Content for Methane + Water and Methane + Ethane + n−Butane + Water Systems Using a New Sampling Device

**ARTICLE** *in* JOURNAL OF CHEMICAL & ENGINEERING DATA · MAY 2005

Impact Factor: 2.04 · DOI: 10.1021/je049615s



**4 AUTHORS:**

Antonin Chapoy
Heriot-Watt University
**105** PUBLICATIONS **1,640** CITATIONS
SEE PROFILE

Amir H. Mohammadi
**549** PUBLICATIONS **4,714** CITATIONS
SEE PROFILE

Bahman Tohidi
Heriot-Watt University
**214** PUBLICATIONS **3,047** CITATIONS
SEE PROFILE

Dominique Richon
Aalto University
**532** PUBLICATIONS **6,495** CITATIONS
SEE PROFILE

# Estimation of Water Content for Methane + Water and Methane + Ethane + *n*-Butane + Water Systems Using a New Sampling Device

**Antonin Chapoy,[†] Amir H. Mohammadi,[‡] Bahman Tohidi,[‡] and Dominique Richon*[,†]**

Centre Energétique et Procédés, Ecole Nationale Supérieure des Mines de Paris, CEP/TEP, 35 Rue Saint Honoré, 77305 Fontainebleau, France, and Centre for Gas Hydrate Research, Institute of Petroleum Engineering, Heriot-Watt University, Edinburgh EH14 4AS, Scotland, U.K.

Experimental data and thermodynamic modeling corresponding to water solubility in methane and in a synthetic gas mixture (94 mol % methane, 4 mol % ethane, and 2 mol % *n*-butane) are reported. Equilibrium data of water content in methane were measured in the (277.8 to 297.9) K temperature range and in the gas mixture in a larger (303.1 to 361.4) K temperature range for pressures up to 4.9 MPa, using a static-analytic apparatus that takes advantage of a new sampling device. The Valderrama modification of the Patel−Teja equation of state with the non-density-dependent mixing rules is used for modeling the fluid phases with previously reported binary interaction parameters. The hydrate phase is modeled by the van der Waals and Platteeuw solid solution theory using previously reported Kihara potential parameters. The new experimental data are in good agreement with the predictions of this model, with a previously developed semiempirical approach, and with some selected experimental data from the literature, demonstrating the reliability of the experimental data and technique and predictive methods used in this work.

## Introduction

Natural gases usually contain significant quantities of water. During production, transportation, and processing, changes in temperature and pressure can lead to water condensation, thus altering the physical state from vapor to condensed water, ice and/or gas hydrates. Accurate data are necessary to develop and validate predictive methods. Unfortunately, data for most natural gas components at low-temperature conditions are scarce.[1]

The main objective of this work is to provide the much needed solubility data at the above-mentioned conditions. These data correspond to an extension of the work done at lower temperatures (down to 248 K) and higher pressures (up to 34.5 MPa) in the frame of the GPA 987 Research Project for the Gas Processors Association (Tulsa, OK). For this purpose, new water content data of the $CH_4 + H_2O$ vapor−liquid binary system and of a gas mixture (94 mol % $CH_4$ + 4 mol % $C_2H_6$ + 2 mol % *n*-$C_4H_{10}$) + $H_2O$ system are reported herein in the (277.8 to 297.9) K temperature range at pressures up to almost 4.4 MPa for the first system and in the (303.1 to 361.4) K temperature range at pressures up to 4.9 MPa for the second system. The compositions of the vapor phase are measured by a gas chromatography (GC) method. The isotherms presented in this work are determined using an apparatus based on a static-analytic method taking advantage of a new electromagnetic capillary sampler.

A thermodynamic model based on the uniformity of fugacity of each component throughout all of the phases is employed to model the phase equilibrium. The Valderrama modification of the Patel−Teja equation of state (VPT-EoS)[2] with the non-density-dependent (NDD) mixing rules[3] is used for predicting the fugacity of components in fluid phases using previously reported binary interaction parameters (BIPs).[4−6] The hydrate phase is modeled by the solid solution theory of van der Waals and Platteeuw[7] using the previously reported Kihara potential parameters.[6] To evaluate the consistency of the new data further, the experimental results are compared with a previously reported semiempirical approach[8] and to other experimental data from the literature. The results are in good agreement, demonstrating the realibility of techniques and predictive tools used for this work.

## Experimental Section

***Materials.*** Methane was purchased from Messer Griesheim with a certified purity greater than 99.995 vol %. Helium from Air Liquide was pure grade with traces of water (3 ppm) and of hydrocarbons (0.5 ppm). The gas mixture, 94% methane, 4% ethane (±2%, i.e., 3.92 to 4.08%), and 2% *n*-butane (± 2%, i.e., 1.96 to 2.04%), was purchased from Messer Griesheim. Deionized water was used after degassing.

***Apparatus and Procedures.*** A summary of the experimental techniques for measuring the water content/water dew point of gases is given elsewhere.[1] The apparatus used in this work (Figure 1) is based on a static-analytic method with vapor-phase sampling, which is similar to that previously described by Chapoy et al.[4,9−12] and Mohammadi et al.[1,5,8,13]

The phase equilibrium is achieved in a cylindrical cell made of sapphire. The cell volume is about 20 $cm^3$, and it can be operated up to 10 MPa between (223.15 and 473.15) K. The cell is immersed in a constant-temperature liquid bath that controls and maintains the desired temperature within ±0.02 K. To perform accurate temperature measurements in the equilibrium cell and to check for thermal gradients, the temperature is measured at two locations corresponding to the vapor and liquid phases through two 100 Ω platinum resistance thermometers (Pt100) connected

* To whom correspondence should be addressed. E-mail: richon@paris.ensmp.fr. Tel: +(33) 1 64 69 49 65. Fax: +(33) 1 64 69 49 68.
† Ecole Nationale Supérieure des Mines de Paris.
‡ Institute of Petroleum Engineering.

10.1021/je049615s CCC: $30.25 
Published on Web 05/19/2005

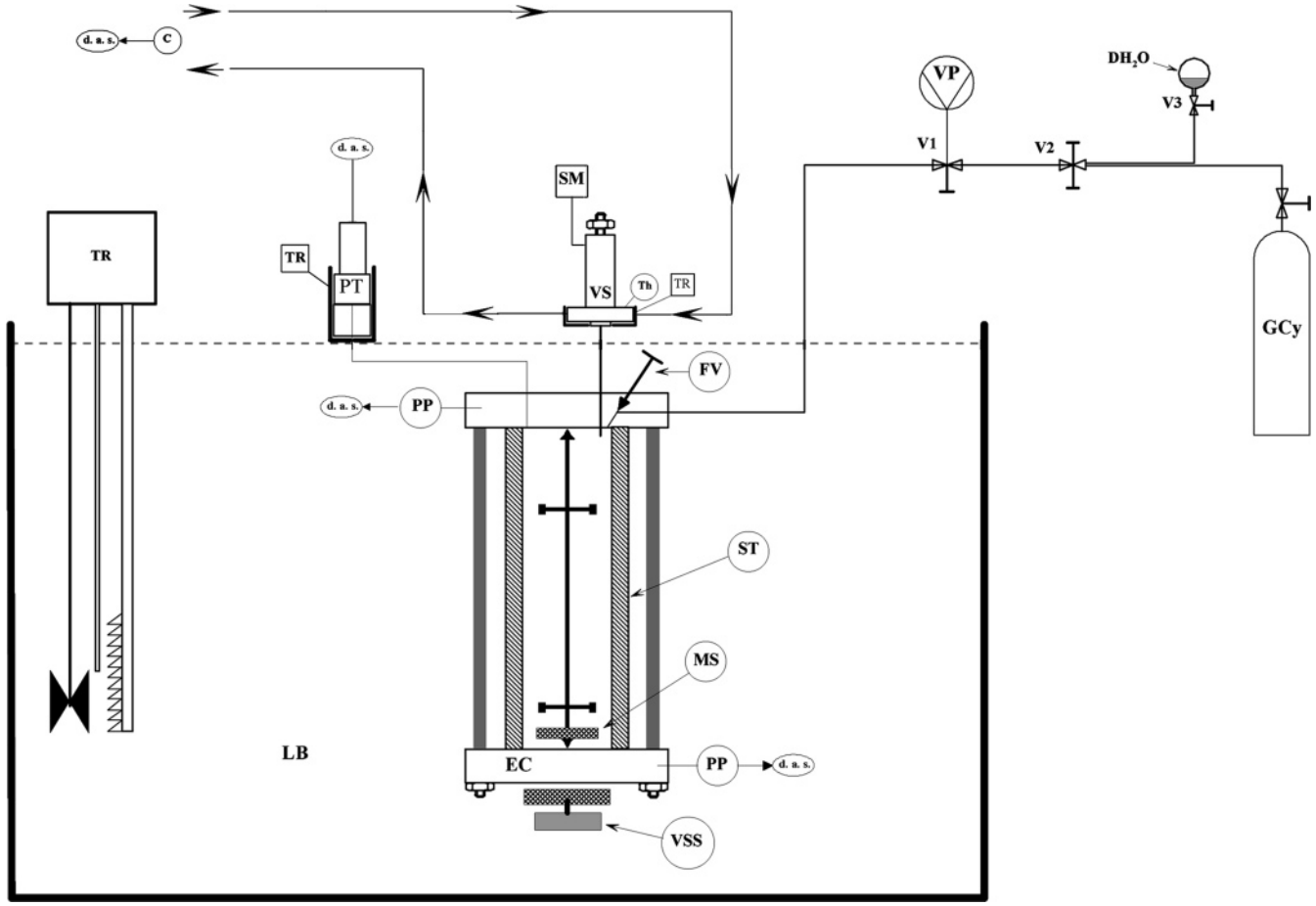


**Figure 1.** Flow diagram of the equipment:[1,4,5,8–12] C, carrier gas; d.a.s, data acquisition system; $DH_2O$, degassed water; EC, equilibrium cell; FV, feeding valve; GCy, gas cylinder (either methane or hydrocarbon mixture); LB, liquid bath; MS, magnetic stirrer; PP, platinum resistance thermometer probe; PT, pressure transducer; SM, sampler monitoring; ST, sapphire tube; Th, thermocouple; TR, temperature regulator; Vi, valve i; VS, vapor sampler; VSS, variable-speed stirrer; VP, vacuum pump.

to an HP data acquisition unit (HP34970A). These two Pt100 thermometers are carefully and periodically calibrated against a 25 Ω reference platinum resistance thermometer (TINSLEY Precision Instruments). The resulting uncertainty is better than ±0.02 K in the (273.15 to 393.15) K range. The 25 Ω reference platinum resistance thermometer was calibrated by the Laboratoire National d'Essais (Paris) on the 1990 International Temperature Scale (ITS 90). Pressure is measured by means of a Druck pressure transducer connected to the HP data acquisition unit (HP34970A); the pressure transducer is maintained at a constant temperature (temperature higher than the highest temperature of the study) by means of a specially made air thermostat, which is controlled using a PID regulator (West, model 6100). The pressure transducer is calibrated against a dead weight pressure balance (Desgranges & Huot 5202S, CP (0.3 to 40) MPa, Aubervilliers, France). Pressure measurement uncertainties are estimated to be within ±1 kPa in the (0.2 to 5) MPa range.

The HP online data acquisition unit is connected to a personal computer through an RS-232 interface. This system allows real-time readings and storage of temperatures and pressures throughout the different isothermal runs. The analytical work was carried out using a GC (Varian model CP-3800) equipped with a thermal conductivity detector (TCD) connected to a data acquisition system fitted with Borwin software (version 1.5 from JMBS, Le Fontanil, France). The analytical column is a Hayesep T 100/120 mesh column (silcosteel tube, length 1.5 m, diameter $^1/_8$ in.).

The FID and TCD were utilized to detect the hydrocarbons and water, respectively. It was repeatedly calibrated by introducing known amounts of the gas mixture through a gas syringe in the injector of the gas chromatograph. The uncertainties of the calculated moles are estimated to be ±2.0% in the ($3.8 \times 10^{-6}$ to $2.0 \times 10^{-5}$) mol range, ±2.2% in the ($1.6 \times 10^{-7}$ to $8.2 \times 10^{-7}$) mol range, and ±3.5% in the ($8.2 \times 10^{-8}$ to $4.1 \times 10^{-7}$) mol range for methane, ethane, and *n*-butane, respectively. Because the water concentration is expected to be very low, calibrating the detectors is very difficult. It is indeed impossible to inject such a small quantity correctly into the chromatograph using syringes. For calibration purposes, a dilutor apparatus is used with a specific calibration circuit. The calibration procedure has been previously described by Chapoy et al.[9,10] and Mohammadi et al.[1,5] The cell of the dilutor is immersed inside a liquid thermoregulated bath. Helium is bubbled through the dilutor cell filled with water to be saturated before entering the chromatograph through an external loop injection valve. In using the dilutor and a loop injection valve, a well-defined amount of water can be injected into the chromatograph. The calculation of the amount of water, $n_w$, is carried out using the equilibrium and mass balance relation given by

$$n_w = \gamma_w^L x_w \frac{P_w^{sat}}{P_{dilutor}} \frac{\varphi_w^{sat}}{\varphi_w^V} \left(\frac{PV}{ZRT}\right)^{loop} \exp\left(\left(\frac{v_w^L}{RT}\right)(P_{dilutor} - P_w^{sat})\right) \quad (1)$$

**Table 1. Critical Properties and Acentric Factors[14]**

| compounds | $P_c$/MPa | $T_c$/K | $v_c$/m$^3$·kmol$^{-1}$ | $\omega$ |
|---|---|---|---|---|
| water | 22.048 | 647.30 | 0.056 | 0.3442 |
| methane | 4.604 | 190.58 | 0.0992 | 0.0108 |
| ethane | 4.880 | 305.42 | 0.1479 | 0.09896 |
| *n*-butane | 3.797 | 425.18 | 0.255 | 0.1931 |

**Table 2. BIPs for the VPT-EoS,[2] and NDD Mixing Rules[3a]**

| systems | $k_{w-g}$[e] | $l^0_{w-g}$[f] | $l^1_{w-g} \times 10^4$[f] |
|---|---|---|---|
| methane+water[b] | 0.5044 | 1.8302 | 51.72 |
| ethane+water[c] | 0.5442 | 1.5629 | 35.23 |
| *n*-butane+water[d] | 0.5800 | 1.6885 | 33.57 |

[a] w, water; g, gas. [b] From Chapoy et al. (2004).[4] [c] From Mohammadi et al. (2004).[5] [d] FromTohidi-Kalorazi (1995).[6] [e] $k_{w-g}$: BIP for the classical mixing rules. [f] $l^0_{w-g}$ and $l^1_{w-g}$: constants for the BIP for the asymmetric term.

**Table 3. Kihara Potential Parameters for Methane, Ethane, and *n*-Butane[6]**

| compounds | α/Å | $\sigma^*$/Å | $\epsilon/k$/K |
|---|---|---|---|
| methane | 0.2950 | 3.2512 | 153.69 |
| ethane | 0.4880 | 3.4315 | 183.32 |
| *n*-butane | 1.0290 | 3.4000 | 195.36 |

α: Kihara hard-core radius. $\sigma$: Collision diameter. $\epsilon$: Characteristic energy. $k$: Boltzmann's constant. $\sigma^* = \sigma - 2\alpha$.

**Table 4. Thermodynamic Reference Properties for Structure-I (sI) and Structure-II (sII) Hydrates**

| properties | sI | sII |
|---|---|---|
| $\Delta\mu_w^0$/J·mol$^{-1}$[g] | 1297[d] | 937[d] |
| $\Delta h_w^0$/J·mol$^{-1}$[a,h] | 1389[d] | 1025[d] |
| $\Delta v_w$/cm$^3$·mol$^{-1}$[b,i] | 3.0[e] | 3.4[e] |
| $\Delta C^0_{pw}$/J·mol$^{-1}$·K$^{-1}$[c,j] | −37.32[f] | −37.32[f] |

[a] In the liquid-water region, subtract 6009.5 J·mol$^{-1}$ from $\Delta h_w^0$. [b] In the liquid-water region, add 1.601 cm$^3$·mol$^{-1}$ to $\Delta v_w$. [c] Values to be used in $\Delta C_{pw} = \Delta C^o_{pw} + 0.179\,(T - T_0)$, where $T_0$ is the reference temperature. [d] From Dharmawardhana et al. (1980).[19] [e] From Parrish and Prausnitz (1972).[20] [f] From Holder et al. (1980).[18] [g] $\Delta\mu_w^0$: Chemical potential difference between the empty hydrate lattice and ice at the ice point and zero pressure. [h] $\Delta h_w^0$: Enthalpy difference between the empty hydrate lattice and ice at the ice point and zero pressure. [i] $\Delta v_w$: Molar volume difference between the empty hydrate lattice and ice/liquid water. [j] $\Delta C^0_{pw}$: Reference heat capacity difference between the empty hydrate lattice and liquid water at 273.15 K. $\Delta C_{pw}$: Heat capacity difference between the empty hydrate lattice and liquid water.

where $\gamma_w^L$ is the activity coefficient of water in the aqueous phase; $x_w$ is the mol fraction of water in the liquid aqueous phase of the dilutor; $P_w^{sat}$ stands for the vapor pressure of water at temperature $T$; $P_{dilutor}$ represents the pressure in the dilutor; $\varphi_w^{sat}$ is the vapor fugacity coefficient of saturated pure water; $\varphi_w^V$ is the vapor fugacity coefficient of water; $P$, $V$, $Z$, and $R$ are the pressure, volume, compressibility factor, and gas constant; the superscript *loop* stands for loop properties; and $v_w^L$ is the molar volume of liquid water at $T$.

It is essential to know precisely the volume and the dead volume (slots between valve ports where the loop is actually fitted) of the sampling valve (volume + dead volume = $V^{loop}$). First, the volume of the external loop is roughly calculated (around 40 μL), and then a calibration with methane as a reference gas using a 50 μL gas syringe is done around the value of the rough estimation. After this careful methane calibration, methane is passed through the sampling valve and injected into the GC. Knowing the number of moles of methane swept into the GC through the previous calibration, the volume and the dead volume of the loop can be estimated to be (35.5 ± 0.1) μL. The experimental accuracy of the TCD calibration for water, from ($7.5 \times 10^{-9}$ to $3.4 \times 10^{-7}$) mol, is estimated to be ±4%.

The sampling is carried out using a new capillary sampler-injector that is connected to the cell through a 0.1 mm internal diameter capillary tube. The withdrawn samples are directly swept by carrier gas to a Varian 3800 gas chromatograph for analysis. The capillary inlet of the sampler is directly in contact with the vapor phase, and the outlet of the capillary is closed by a microneedle, whose opening is controlled by an electromagnet, when the open outlet of the capillary is in contact with the carrier gas through the expansion room. This room is crossed by the gas, which sweeps the sample to be analyzed to the GC. The sampler allows direct sampling at working pressures without disturbing the cell equilibrium. The mass of the sample can be varied continuously from 0.01 up to several milligrams. The expansion room of the sampler is heated independently from the equilibrium cell to allow the samples to remain as a vapor.

The equilibrium cell and its loading lines are evacuated down to 0.1 Pa prior to the introduction of about 5 cm$^3$ of degassed water. Then, methane or a gaseous hydrocarbon mixture is introduced into the cell directly from the commercial cylinder (through preliminary evacuated transfer lines) to a pressure level corresponding to the pressure of the first measurement. More gas is introduced after each sampling and analysis step up to given pressures. After each introduction of gas into the cell, efficient stirring is started, and pressure is stabilized within a few minutes; measurements are performed only when pressure is constant within experimental uncertainty. (Furthermore, pressure is ensured to remain constant in all sample analyzes.)

For each equilibrium condition, at least 10 samples are withdrawn from the vapor phase using the sampler and analyzed to check for measurement repeatability. Because the volume of the withdrawn samples is very small (typically less than 1 mg) compared to the total mass inside the equilibrium cell (more than 5 g), it is possible to withdraw many samples without significantly disturbing the studied phase equilibrium.

## Thermodynamic Model

***Pure Compound Properties.*** The critical temperature ($T_C$), critical pressure ($P_C$), critical volume ($v_C$), and acentric factor ($\omega$) for each of the pure compounds are provided in Table 1.[14]

***Description of the Model.*** A thermodynamic model based on the uniformity of the fugacity of each component throughout all of the phases[15,16] is used to model the phase equilibrium. A detailed description of the model for predicting the water content of gases is given elsewhere.[1] Briefly, the VPT-EoS[2] with the NDD mixing rules[3] is employed in calculating fugacities in all fluid phases. This combination has proved to be a strong tool in modeling systems with polar and nonpolar compounds[3] and in modeling phase behavior in water−natural gas component systems.[1,4,5,11−13,17] The BIPs for methane + water, ethane + water, and *n*-butane + water are those reported previously and listed in Table 2.[4−6] All of the BIPs for hydrocarbon + hydrocarbon systems were set to zero.

The fugacity of ice is rigorously calculated by correcting the saturation fugacity of water at the same temperature using the Poynting correction.[15,16] The hydrate phase is modeled by the solid solution theory of van der Waals and Platteeuw.[7] The Kihara potential parameters with a spheri-

**Table 5. Experimental and Predicted Water Contents (mole fraction) in Methane + Water and Gas Mixture + Water Systems**

| | | | semiempirical approach [8] | | thermodynamic model [1] | |
|---|---|---|---|---|---|---|
| *T*/K | *P*/MPa | experimental water content ($\times 10^4$) | predicted water content ($\times 10^4$) | AD % | predicted water content ($\times 10^4$) | AD % |
| | | | $CH_4 + H_2O$ | | | |
| 277.8 | 0.491 | 17.3 | 17.7 | 2.3 | 17.7 | 2.3 |
| 277.8 | 1.081 | 8.30 | 8.30 | 0.0 | 8.28 | 0.2 |
| 277.8 | 2.196 | 4.36 | 4.31 | 1.1 | 4.29 | 1.6 |
| 277.8 | 3.136 | 3.21 | 3.16 | 1.6 | 3.14 | 2.2 |
| 279.3 | 1.178 | 8.61 | 8.49 | 1.4 | 8.47 | 1.6 |
| 282.9 | 0.493 | 26.4 | 25.1 | 4.9 | 25.0 | 5.3 |
| 282.9 | 0.688 | 18.3 | 18.1 | 1.1 | 18.1 | 1.1 |
| 283.0 | 1.081 | 12.2 | 11.8 | 3.3 | 11.8 | 3.3 |
| 282.9 | 1.458 | 9.26 | 8.87 | 4.2 | 8.84 | 4.5 |
| 283.0 | 2.822 | 5.30 | 4.91 | 7.4 | 4.89 | 7.7 |
| 283.0 | 4.374 | 3.13 | 3.40 | 8.6 | 3.38 | 8.0 |
| 287.7 | 0.993 | 18.5 | 17.4 | 5.9 | 17.4 | 5.9 |
| 287.7 | 1.985 | 9.33 | 9.12 | 2.3 | 9.09 | 2.6 |
| 287.7 | 2.393 | 7.75 | 7.71 | 0.5 | 7.67 | 1.0 |
| 292.7 | 0.976 | 25.2 | 24.3 | 3.6 | 24.3 | 3.6 |
| 292.7 | 2.690 | 9.26 | 9.49 | 2.5 | 9.44 | 1.9 |
| 292.7 | 2.735 | 9.08 | 9.35 | 3.0 | 9.31 | 2.5 |
| 292.7 | 3.667 | 7.03 | 7.25 | 3.1 | 7.21 | 2.6 |
| 297.6 | 1.008 | 31.0 | 31.7 | 2.3 | 31.7 | 2.3 |
| 297.5 | 2.342 | 14.4 | 14.3 | 0.7 | 14.3 | 0.7 |
| 297.9 | 3.675 | 10.0 | 9.87 | 1.3 | 9.82 | 1.8 |
| 297.6 | 3.865 | 8.76 | 9.29 | 6.1 | 9.25 | 5.6 |
| | | | Gas Mixture + $H_2O$ | | | |
| 303.1 | 0.511 | 84.7 | 84.6 | 0.1 | 84.5 | 0.2 |
| 303.9 | 1.068 | 43.0 | 43.3 | 0.7 | 43.2 | 0.5 |
| 303.1 | 2.415 | 19.8 | 19.3 | 2.5 | 19.3 | 2.5 |
| 303.0 | 3.661 | 12.7 | 13.3 | 4.7 | 13.2 | 3.9 |
| 322.0 | 0.526 | 226 | 226 | 0.0 | 226 | 0.0 |
| 321.8 | 1.103 | 106 | 109 | 2.8 | 109 | 2.8 |
| 322.0 | 1.924 | 64.4 | 64.6 | 0.3 | 64.6 | 0.3 |
| 321.9 | 3.114 | 39.6 | 41.3 | 4.3 | 41.3 | 4.3 |
| 321.8 | 4.174 | 30.5 | 31.7 | 3.9 | 31.7 | 3.9 |
| 332.6 | 0.510 | 397 | 387 | 2.5 | 388 | 2.3 |
| 332.7 | 1.523 | 134 | 134 | 0.0 | 135 | 0.7 |
| 333.0 | 2.915 | 72.2 | 74.0 | 2.5 | 74.4 | 3.0 |
| 332.9 | 4.902 | 45.3 | 46.4 | 2.4 | 46.7 | 3.1 |
| 347.3 | 0.567 | 689 | 666 | 3.3 | 670 | 2.8 |
| 347.1 | 1.534 | 253 | 250 | 1.2 | 252 | 0.4 |
| 347.3 | 2.660 | 151 | 150 | 0.7 | 151 | 0.0 |
| 347.2 | 4.115 | 99 | 100 | 1.4 | 101 | 2.4 |
| 361.2 | 0.954 | 698 | 696 | 0.3 | 705 | 1.0 |
| 361.4 | 1.740 | 401 | 391 | 2.5 | 398 | 0.7 |
| 361.3 | 3.050 | 236 | 229 | 3.0 | 233 | 1.3 |
| 361.0 | 4.599 | 152 | 155 | 2.0 | 159 | 4.6 |

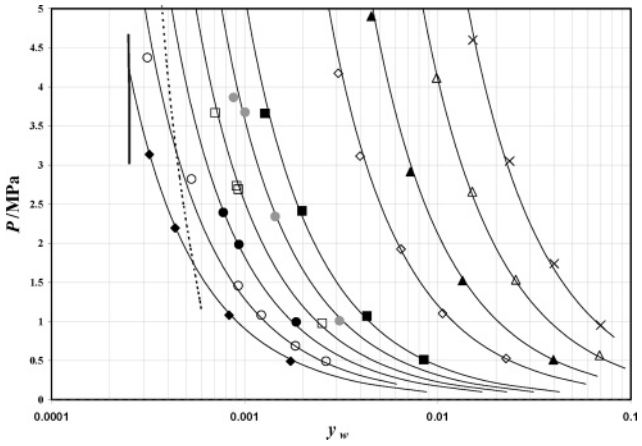


**Figure 2.** Water content, $y_w$ (mol fraction), in the gas (or vapor) phase in the methane + water system and the methane + ethane + *n*-butane + water system. $CH_4$+$H_2O$: ◆, 277.8 K; ○, 282.9 K; ●, 287.7 K; □, 292.7 K; gray circle, 297.6 K. $CH_4$+$C_2H_6$+*n*-$C_4H_{10}$+$H_2O$: ■, 303.1 K; ◇, 321.9 K; ▲, 332.9 K; △, 347.2 K; ×, 361.2 K. Dashed line: water content at mixture-hydrate-formation conditions. Thick solid line: water content at methane-hydrate-formation conditions.

cal core are selected to describe the potential function. These parameters are taken from Tohidi-Kalorazi[6] (Table 3). The heat capacity difference between the empty hydrate and the pure liquid water is calculated using the equation proposed by Holder et al.[18] The reference properties used are summarized in Table 4.

## Results and Discussion

The new experimental water content data are reported in Table 5 and are plotted in Figure 2 for both systems. These data are compared with the results of the thermodynamic model described in the last section[1] and a previously reported semiempirical approach.[8] The agreement between the experimental and predicted data is good, with absolute deviation (AD) values in the (0.2 to 8.0)% range for the thermodynamic model[1] and in the (0 to 8.6)% range for the semiempirical approach[8] applied to the methane+water system. The AD values for the gas mixture+water system are between (0 and 4.6)% for the thermodynamic model[1] and between (0 and 4.7)% for the semiempirical approach.[8] The average absolute deviations (AADs) among all of the experimental and predicted data for the methane+water system are identical (3.1%) for both the thermodynamic model[1] and the semiempirical approach.[8] The AADs among all of the experimental and predicted data for the gas mixture+water system are also identical (1.7%) for both the thermodynamic model[1] and the semiempirical approach.[8] For extended evaluation, a comparison is also

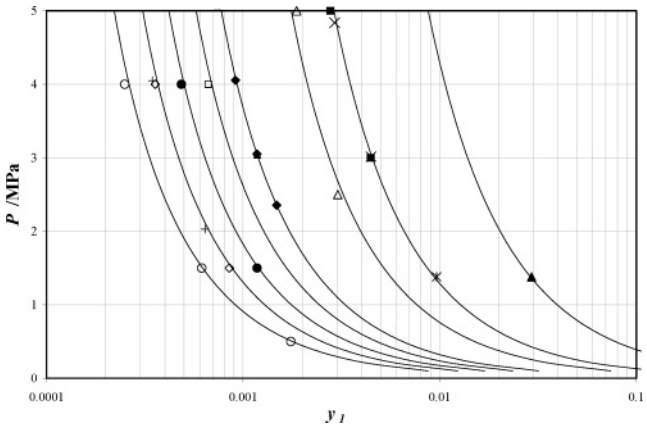


**Figure 3.** Water content, $y_w$ (mol fraction), in the gas (or vapor) phase in the methane + water system. Solid line: water content in the gas phase of the methane + water system. ○, 278.15 K from Althaus (1999);[21] ◇, 283.15 K from Althaus (1999);[21] +, 283.15 K from Kosyakov et al. (1982);[22] ●, 288.15 K from Althaus (1999);[21] □, 293.15 K from Althaus (1999);[21] ◆, 298.15 K from Rigby and Prausnitz (1968);[23] gray triangle, 298.15 K from Yarym-Agaev et al. (1985);[25] −, 298.15 K from Yokoyama et al. (1988);[24] △, 313.15 K from Yarym-Agaev et al. (1985);[25] ×, 323.15 K from Rigby and Prausnitz (1968);[23] ■, 323.15 K from Yokoyama et al. (1988);[24] *, 323.15 K from Gillespie and Wilson (1982);[26] ▲, 348.15 K from Gillespie and Wilson (1982).[26]

made between the new data and some selected data from the literature. The results at all conditions are consistent with those of all of the authors, as illustrated in Figure 3. The agreement between the new experimental data, predictions of the thermodynamic model[1] and semiempirical approach,[8] and the selected literature data demonstrates the reliability of the experimental data and technique and the predictive methods used in this work.

## Conclusions

New experimental data on the water content of the methane + water and of the gas mixture (94% methane + 4% ethane + 2% *n*-butane) + water systems were generated in the (277.8 to 297.9) K and (303.1 to 361.4) K temperature ranges, respectively, and for pressures up to about 5 MPa by using a static-analytic method with equipment that takes advantage of a new high-pressure capillary sampler. The new experimental data are compared to predictions of a previously reported thermodynamic model and a semiempirical approach and to selected experimental data from the literature. Good agreement is observed, demonstrating the reliability of the experimental data and technique and predictive methods used in this work.

## Literature Cited

(1) Mohammadi, A. H.; Chapoy, A.; Richon, D.; Tohidi, B. Experimental Measurement and Thermodynamic Modeling of Water Content in Methane and Ethane Systems. *Ind. Eng. Chem. Res.* **2004**, *43*, 7148−7162.

(2) Valderrama, J. O. A generalized Patel-Teja equation of state for polar and non-polar fluids and their mixtures. *J. Chem. Eng. Jpn* **1990**, *23*, 87−91.

(3) Avlonitis, D.; Danesh, A.; Todd, A. C. Prediction of VL and VLL equilibria of mixtures containing petroleum reservoir fluids and methanol with a cubic EoS. *Fluid Phase Equilib.* **1994**, *94*, 181−216.

(4) Chapoy, A.; Mohammadi, A. H.; Richon, D.; Tohidi, B. Gas solubility measurement and modeling for methane−water and methane−ethane−*n*-butane−water systems at low-temperature conditions. *Fluid Phase Equilib.* **2004**, *220*, 113−121.

(5) Mohammadi, A. H.; Chapoy, A.; Tohidi, B.; Richon, D. Measurements and Thermodynamic Modeling of Vapor−Liquid Equilibria in Ethane−Water Systems from 274.26 to 343.08 K. *Ind. Eng. Chem. Res.* **2004**, *43*, 5418−5424.

(6) Tohidi-Kalorazi, B. Gas Hydrate Equilibria in the Presence of Electrolyte Solutions. Ph.D. Thesis, Heriot-Watt University, Edinburgh, U.K., 1995.

(7) van der Waals, J. H.; Platteeuw, J. C. Clathrate Solutions. *Adv. Chem. Phys*. **1959**, *2*, 1−57.

(8) Mohammadi, A. H.; Chapoy, A.; Tohidi, B.; Richon, D. A Semiempirical Approach for Estimating the Water Content of Natural Gases. *Ind. Eng. Chem. Res.* **2004**, *43*, 7137−7147.

(9) Chapoy, A.; Coquelet, C.; Richon, D. Solubility measurement and modeling of water in the gas phase of the methane/water binary system at temperatures from 283.08 to 318.12 K and pressures up to 34.5 MPa. *Fluid Phase Equilib.* **2003**, *214*, 101−117.

(10) Chapoy, A.; Coquelet, C.; Richon, D. Measurement of the Water Solubility in the Gas Phase of the Ethane + Water Binary System near Hydrate Forming Conditions. *J. Chem. Eng. Data* **2003**, *48*, 957−966.

(11) Chapoy, A.; Mohammadi, A. H.; Tohidi, B.; Richon, D. Gas Solubility Measurement and Modeling for the Nitrogen + Water System from 274.18 K to 363.02 K. *J. Chem. Eng. Data* **2004**, *49*, 1110−1115.

(12) Chapoy, A.; Mokraoui, S.; Valtz, A.; Richon, D.; Mohammadi, A. H.; Tohidi, B. Solubility measurement and modeling for the system propane-water from 277.62 to 368.16 K. *Fluid Phase Equilib.* **2004**, *226*, 255−263.

(13) Mohammadi, A. H.; Chapoy, A.; Tohidi, B.; Richon, D. Water Content Measurement and Modeling in the Nitrogen + Water System. *J. Chem. Eng. Data* **2005**, *50*, 541−545.

(14) Avlonitis, D. A. Multiphase Equilibria in Oil-Water Hydrate Forming Systems. M.Sc. Thesis, Heriot-Watt University, Edinburgh, U.K., 1988.

(15) Avlonitis, D. A. Thermodynamics of Gas Hydrate Equilibria. Ph.D. Thesis, Heriot-Watt University, Edinburgh, U.K., 1992.

(16) Tohidi, B.; Burgass, R. W.; Danesh, A.; Todd, A. C. Hydrate Inhibition Effect of Produced Water, Part 1. Ethane and Propane Simple Gas Hydrates. *SPE 26701*, *Proceedings of the SPE Offshore Europe 93 Conference,* 1993; pp 255−264.

(17) Chapoy, A.; Mohammadi, A. H.; Chareton, A.; Tohidi, B.; Richon, D. Measurement and Modeling of Gas Solubility and Literature Review of the Properties for the Carbon Dioxide−Water System. *Ind. Eng. Chem. Res.* **2004**, *43*, 1794−1802.

(18) Holder, G. D.; Corbin, G.; Papadopoulos, K. D. Thermodynamic and Molecular Properties of Gas Hydrates from Mixtures Containing Methane, Argon, and Krypton. *Ind. Eng. Chem. Fundam*. **1980**, *19*, 282−286.

(19) Dharmawardhana, P. B.; Parrish, W. R.; Sloan, E. D. Experimental Thermodynamic Parameters for the Prediction of Natural Gas Hydrate Dissociation Conditions. *Ind. Eng. Chem. Fundam*. **1980**, *19*, 410−414.

(20) Parrish, W. R.; Prausnitz, J. M. Dissociation Pressures of Gas Hydrates Formed by Gas Mixtures. *Ind. Eng. Chem. Process Des. Dev*. **1972**, *11*, 26−35.

(21) Althaus, K. *Fortschr.−Ber. VDI, Reihe 3* **1999**, 350 (in German). Oellrich, L. R.; Althaus, K. GERG − Water Correlation (GERG Technical Monograph TM14) Relationship Between Water Content and Water Dew Point Keeping in Consideration the Gas Composition in the Field of Natural Gas. *Fortschr.−Ber. VDI, Reihe 3* **2000** (in English).

(22) Kosyakov, N. E.; Ivchenko, B. I.; Krishtopa, P. P. Solubility of moisture in compressed gases at low temperatures. *Zh. Prikl. Khim.* **1982**, *68*, 33−36.

(23) Rigby, M.; Prausnitz, J. M. Solubility of Water in Compressed Nitrogen, Argon, and Methane. *J. Phys. Chem.* **1968**, *72*, 330−334.

(24) Yokoyama, C.; Wakana, S.; Kaminishi, G. I.; Takahashi, S. Vapor−Liquid Equilibria in the Methane−Diethylene Glycol−Water System at 298.15 and 323.15 K. *J. Chem. Eng. Data* **1988**, *33*, 274−276.

(25) Yarym-Agaev, N. L.; Sinyavskaya, R. P.; Koliushko, I. I.; Levinton, L. Ya. *Zh. Prikl. Khim.* **1985**, *58*, 165−168 (in Russian).

(26) Gillespie, P. C.; Wilson, G. M. Vapor-Liquid and Liquid−Liquid Equilibria: Water−Methane, Water−Carbon Dioxide, Water−Hydrogen Sulfide, Water−nPentane, Water−Methane−nPentane. GPA Research Report 48; Gas Processors Association: Tulsa, OK, April 1982,.

Received for review November 3, 2004. Accepted April 13, 2005. The financial support of the European Infrastructure for Energy Reserve Optimization (EIERO) and the Gas Processors Association (GPA) provided the opportunity for this joint work, which is gratefully acknowledged.

JE049615S